

Magnetic Resonance Image Guided Transurethral Ultrasound Prostate Ablation: A Preclinical Safety and Feasibility Study with 28-Day Followup

Mathieu Burtnyk,^{*,†} Tracy Hill, Heather Cadieux-Pitre and Ian Welch

From Profound Medical, Inc., Toronto and Animal Care and Veterinary Services, Western University (TH, HC-P, IW), London, Ontario, Canada

Purpose: We determine the safety and feasibility of magnetic resonance image guided transurethral ultrasound prostate ablation using active temperature feedback control in a preclinical canine model with 28-day followup.

Materials and Methods: After a long acclimatization period we performed ultrasound treatment in 8 subjects using the magnetic resonance image guided TULSA-PRO™ transurethral ultrasound prostate ablation system. Comprehensive examinations and observations were done before and throughout the 28-day followup, including assessment of clinically significant treatment related adverse events. In addition to gross pathology evaluation, extensive histopathological analysis was done to assess cell kill inside and outside the prostate. We evaluated prostate conformal heating by comparing the spatial difference between the treatment plan and the 55C isotherm measured on magnetic resonance imaging thermometry acquired during treatment. These findings were confirmed on contrast enhanced magnetic resonance imaging immediately after treatment and at 28 days.

Results: Clinically there were no adverse events in any of the 8 subjects throughout the 28-day followup. All subjects had normal urinary and bowel function. Gross necropsy and histology confirmed that the intended thermal cell kill was confined to the prostate. No surrounding tissue was damaged, including the rectum and the external urinary sphincter. Conformal heating was achieved with an average -0.9 mm accuracy and 0.9 mm precision. Contrast enhanced magnetic resonance imaging and histological analysis confirmed tissue ablation in targeted areas of the prostate. Urethral tissue was spared from thermal damage.

Conclusions: Magnetic resonance image guided transurethral ultrasound is a safe, feasible procedure for accurate and precise conformal thermal ablation of prostate tissue, as demonstrated in a preclinical model with 28-day followup.

Abbreviations and Acronyms

CEM43 = cumulative equivalent minutes at 43C

CE-MRI = contrast enhanced MRI

DSC = dice similarity coefficient

MRI = magnetic resonance imaging

NPV = nonperfused volume

PS = positioning system

RFE = radio frequency electronics

UA = ultrasound applicator

Accepted for publication November 18, 2014.
Study received institutional animal care committee approval.

Supported by Profound Medical, Inc.

* Correspondence: Profound Medical, Inc., 3080 Yonge St., Suite 4040, Toronto, Ontario M4N 3N1, Canada (telephone: 416-565-2903; FAX: 647-847-3739; e-mail: mburtnyk@profoundmedical.com).

† Financial interest and/or other relationship with Profound Medical.

Key Words: prostatic neoplasms; high intensity focused ultrasound ablation; magnetic resonance imaging, interventional; equipment and supplies; dogs

PROSTATE cancer, the most prevalent cancer in men in economically developed countries, is now recognized as one of the principal medical problems

facing the male population.¹ While conventional treatments for organ confined prostate cancer such as surgery and radiation provide good

control of localized disease, they leave many men with significant long-term complications that affect urinary, bowel and sexual function, which can significantly decrease quality of life.^{2,3} This is increasingly problematic since now younger men who are screened for prostate cancer and in whom continence and potency are of major concern are faced with earlier detection of less severe disease.^{4,5} Thus, the quandary is how to proceed due to a lack of intervention options to treat the disease but not cause substantial, lifelong side effects.

To address this shortcoming in the management of localized prostate cancer there is strong interest in developing new therapies that can provide effective treatment of the disease with low morbidity. MRI guided transurethral ultrasound ablation is a novel, minimally invasive technology that ablates prostate tissue accurately and precisely using real-time active MRI temperature feedback control (fig. 1).⁶ A transurethral device delivers high intensity ultrasound directly into the prostate, quickly raising temperatures to the point of thermal coagulation.⁷⁻¹⁰ MRI thermometry measurements acquired in real time during treatment are applied by a control algorithm to adjust the ultrasound output (power, frequency and rotation rate) and conform ablation volume to the specific prostate

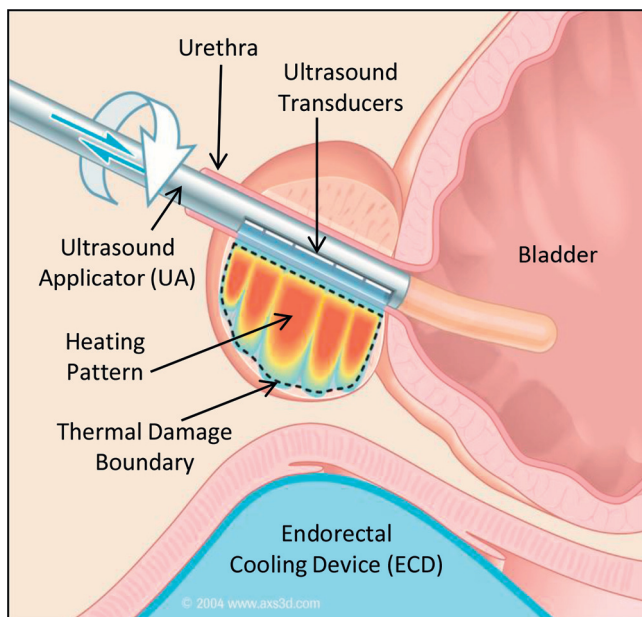


Figure 1. MRI guided transurethral ultrasound prostate ablation. UA emits directional but not focused ultrasound directly into adjacent prostate tissue. Note 5 ultrasound transducer elements but TULSA-PRO includes 10. Under active MRI thermometry temperature feedback control ultrasound power and frequency, and UA rotation rate are adjusted during treatment to accurately and precisely conform thermal ablation region to prostate.

geometry of the patient.¹¹ This decreases possible damage to important surrounding anatomy, such as the rectum, urinary sphincters and neurovascular bundles.¹²

Previous *in vivo* canine studies demonstrated the capability of generating thermal patterns that conform to predetermined target volumes¹³⁻¹⁷ with 1 to 2 mm accuracy and precision.^{14,15} Comprehensive histological analysis revealed the close relationship between acute 100% cell kill and a critical temperature threshold of 55°C (on the order of 1 mm), and the peripheral region of enhancement surrounding the NPV on CE-MRI immediately after treatment (on the order of 3 mm).^{14,15,18} Delayed cell kill at 48 hours migrated 1 to 3 mm beyond the acute cell kill volume.^{14,18}

Recently Sommer et al examined late coagulation effects at 31 days in 2 canine subjects treated with a transurethral ultrasound device designed for benign prostatic hyperplasia with passive MRI thermometry monitoring of the ablation.¹⁷ Complete apparent resorption of ablated tissue with the formation of cystic regions containing fluid was observed along with complete preservation of urethral tissue.

In an initial clinical feasibility study Chopra et al used registered histology to validate the ability to accurately coagulate targeted subvolumes (less than 30% of the prostate) in 8 patients who underwent radical prostatectomy immediately after ultrasound treatment.⁶ Although the study confirmed preclinical findings, the timing of radical prostatectomy prevented interpretation of treatment related adverse events.

We report the findings of what is to our knowledge the first preclinical study with long-term 28-day followup designed to evaluate the safety and feasibility of MRI guided transurethral ultrasound prostate ablation using active temperature feedback control. This study had certain objectives and end points. 1) In terms of safety we determined the onset of clinically significant treatment related adverse events and assessed thermal damage to tissue outside the prostate. 2) In terms of function we evaluated the effect of treatment on urinary and bowel function. 3) In terms of feasibility we quantitatively analyzed the conformal heating and ablation of prostate tissue using MRI thermometry acquired during treatment and performed qualitative assessment by histology 28 days after treatment.

MATERIALS AND METHODS

The study was done at the Department of Animal Care and Veterinary Services, Western University, in accordance with FDA (Food and Drug Administration)

21 CFR (Code of Federal Regulations) Part 58—Good Laboratory Practice for Nonclinical Laboratory Studies and CCAC (Canadian Council on Animal Care) guidelines. Approval for the experiments was obtained from the institutional animal care committee.

Protocol Summary

Eight normal intact male canines served as experimental subjects. After a long acclimatization period (greater than 1 month) perineal urethrostomy was performed to allow insertion of a rigid transurethral device in the prostate. Two weeks postoperatively subjects were anesthetized and underwent ultrasound treatment using the TULSA-PRO transurethral ultrasound prostate ablation system. Anesthesia consisted of premedication with acepromazine, torbutrol and glycopyrrolate, induction with ketamine and valium, and maintenance on isoflurane gas. After placing an indwelling urethral catheter subjects were recovered and monitored daily. Two weeks after treatment the urinary catheter was removed. If subjects pulled out the catheter before this time, the study veterinarian determined whether recatheterization was necessary. Physical examinations, observations, blood studies, urinalysis and fecal occult blood tests were performed before and throughout the study followup, including assessment of clinically significant treatment related adverse events. At the study end point of 4 weeks (28 days) after treatment subjects were anesthetized, imaged by MRI and sacrificed by a sodium pentobarbital overdose. Along with gross pathology extensive histopathological analysis was done to assess cell kill inside and outside the prostate.

MRI Guided Transurethral Ultrasound Ablation

The TULSA-PRO consists of a transurethral UA, an endorectal cooling device, a linear and rotational PS, a RFE, a fluid circuit and a console that incorporates custom treatment software and a proprietary temperature feedback control algorithm.

The rigid cylindrical UA includes an acoustic window with a linear array of 10 planar transducer elements that emit directional (but not focused) high intensity ultrasound energy directly into the prostate. Each transducer is $4 \times 5 \text{ mm}^2$ (50 mm maximum prostatic urethra length) and has an output of up to 4 and 2 acoustic W (spatial average and temporal average) at approximately 4 and 14 MHz, respectively. The RFE supplies electric power without interfering with MRI. The PS holds the UA and provides automated linear translations to align the transducers precisely with the prostate and avoid heating the external urinary sphincter. The PS also provides controlled rotation of the UA to sweep an entire volume and conform thermal ablation to the prostate. The fluid circuit flows water to the UA and endorectal cooling device to cool the urethra and rectum, respectively. The treatment console incorporates custom software to plan treatment, monitor thermal therapy delivery, analyze spatial temperature changes in real time, implement the temperature feedback algorithm and control the RFE and the PS (ultrasound power and frequency, and UA rotation). Treatment was performed on a 3 Tesla Tim Trio MRI device (Siemens™) with multi-channel spine and body matrix coils.

Ultrasound treatment involves conformal thermal ablation of prostate tissue with a target volume determined and drawn on high resolution MRI planning images (T2 turbo spin-echo, oblique axial, sagittal and coronal, echo time/repetition time 52/3,000 milliseconds, 26 cm field of view and $1 \times 1 \times 2.5 \text{ mm}^3$ voxels). The target region was defined to within 6 mm of the prostate capsule, allowing measurement of thermal gradients beyond the target as well as histological analysis of delayed cell kill, which can only be measured in the prostate. Since ultrasound is not focused, the highest temperatures are located near the UA. Therefore, heating the outer boundary of the target region to 55C results in acute thermal coagulation of the entire target volume. Delayed cell kill, which is expected to migrate outward an additional 1 to 3 mm,^{14,15,18} correlates approximately with a Sapareto-Dewey¹⁹ thermal dose of 240 CEM43 or a maximum temperature threshold of 52C. The feedback control algorithm maintains maximum temperatures below 100C to avoid boiling.

Real-time MRI thermometry based on the water proton resonance frequency shift was acquired during ultrasound treatment to measure temperature changes in the prostate noninvasively²⁰ (echo planar, oblique axial, fat saturated, echo time/repetition time 9.5/231 milliseconds, $22 \times 26 \text{ cm}^2$ field of view, $2 \times 2 \times 4 \text{ mm}^3$ and 12 slices with a 1 mm gap). Oblique-axial MRI thermometry and high resolution planning images were centered on each ultrasound transducer element. Before treatment subjects were administered a gastrointestinal antispasmodic drug (20 mg Buscopan®) intravenously to eliminate rectal peristaltic motion, which can cause motion artifact on MRI thermometry. After treatment a gadolinium contrast agent (0.1 mmol/kg Magnevist®) was administered. CE-MRI was performed to confirm acute ablation and visualize the peripheral region of enhancement surrounding the NPV.

Conformal heating of the prostate was evaluated quantitatively using 3 measures of targeting accuracy, defined as the spatial difference between the target region and the 55C isotherm measured on MRI thermometry. Targeting accuracy DSC,²¹ which is unitless with a range of 0 to 1, is a statistical validation metric that measures the degree of spatial overlap between 2 regions. It is determined by the equation, $DSC(A,B) = 2(A \cap B)/(A + B)$, and has been used to evaluate spatial accuracy in brain laser thermal therapy²² and neuroradiology.²³ Targeting accuracy linear measures the accuracy (mean) and precision (SD) of the spatial difference as sampled across each treatment slice. Targeting accuracy volume represents the amount of tissue at 55C or greater outside the target region and at less than 55C inside the target region. It is expressed as a percent of target volume. Since temperature gradients are difficult to resolve in a MRI thermometry voxel, targeting accuracy volume is calculated relative to the target region $\pm 1 \text{ mm}$ margin or half of the in-plane voxel dimension.²⁴

Histology

In each subject the whole specimen was removed en bloc (prostate, bladder, urethra, rectum, vas deferens and corpus cavernosum) to observe any injury caused by

ultrasound treatment outside the prostate and to adjacent organs. Specimens were fixed in 10% neutral buffered formalin solution for a minimum of 7 days. At that time they were sectioned transverse to the urethra in 5 mm blocks, loaded in an automated tissue processor and embedded in paraffin using ASP300 and EG1150H devices (Leica Biosystems, Buffalo Grove, Illinois). Each tissue block was sectioned using a RM2255 rotary microtome (Leica Biosystems) to produce a 5 μ m slide, which was stained with hematoxylin and eosin. This method provided histological information corresponding to approximately the same plane and spacing as the MRI thermometry acquired during treatment. All histology slides were examined by the study veterinary pathologist with a BX41 light microscope (Olympus®). The pathologist recorded comprehensive descriptions of any cellular damage (thermal and nonthermal) and abnormal findings inside and outside the prostate, including the urethra and the external urethral sphincter. Extensive histological analysis was done to assess the extent and shape of treatment related damage in the prostate. Additionally, the prostate histology slides were digitized using a ScanScope® XT System. Cell kill regions were annotated graphically by the veterinary pathologist using ImageScope™.

Conformal thermal ablation was confirmed by qualitatively correlating MRI thermometry measurements (day 0) to CE-MRI acquired immediately after treatment (day 0) and at study completion (day 28) as well as to histological findings (day 28). Significant changes in prostate volume and shape at 28 days precluded a meaningful quantitative correlation between temperature and histology.

RESULTS

Safety and Function

Clinically there was no adverse event in any of the 8 subjects throughout the 28-day followup. All

subjects had normal urinary and bowel function as evidenced by direct observation of normal purposeful urination and defecation, respectively. Of particular clinical relevance was absent fecal and urinary incontinence and retention, which would have been identified during regular monitoring. This finding was consistent regardless of when the urinary catheter was removed, including in 1 subject that removed the catheter 4 days after treatment (average 9, range 4 to 14). Gross necropsy and histology confirmed in all subjects that the intended thermal cell kill was confined to the prostate and no surrounding tissue was damaged. Consistent with functional observations, no damage was observed to the rectum or external urinary sphincter.

However, hematological and biochemical findings were out of the normal range. These findings were attributable to the contrived nature of the model and most specifically to the need for a large perineal urethrostomy immediately adjacent to the anus, as discussed.

Feasibility

Highly conformal temperature control was achieved in vivo, for example in subject 7 (fig. 2). The acute ablation heating pattern at 55C or greater was shaped to the target volume with an average accuracy and precision of -0.9 and 0.9 mm, respectively, which was less than the in-plane MRI thermometry voxel dimension of 2×2 mm². The average DSC was 0.90. Over and under targeted volumes were less than 1% and 7%, respectively. Results in subject 1 were excluded from these averages due to multiple technical failures, including a lower than anticipated ultrasound power output and high

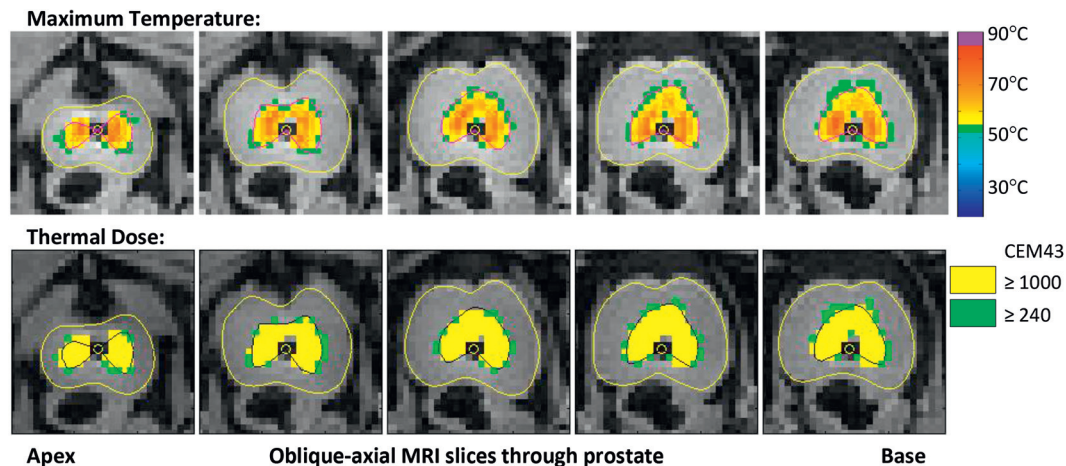


Figure 2. Representative maximum temperature and thermal dose distributions produced in subject 7 prostate show accurate and precise temperature control. Anatomical image overlays represent temperatures of 52C or greater and doses of 240 CEM43 or greater. Yellow areas represent acute thermal coagulation at 55C or greater, or 1,000 CEM43 or greater. Green areas represent estimates of delayed damage at 52C or greater, or 240 CEM43 or greater. Pink and black outlines indicate target boundary. Yellow outline indicates prostate boundary.

thermometry measurement noise. The table lists targeting accuracy results in all subjects.

Delayed cell kill estimated using a thermal dose of 240 CEM43 or greater did not extend beyond 4 mm from the target region, consistent with histology and necropsy observations on and outside the prostate capsule. The mean \pm SD thermal gradient extending from 55C (acute cell kill) to 240 CEM43 (delayed cell kill) was 2.0 ± 0.7 mm (range 0.4 to 4.5). This was in agreement with the acute delayed cell kill margin described in the literature^{14,18} and with thermal gradients predicted by numerical simulations.

Histology confirmed that target volumes were ablated, in agreement with the thermal patterns measured on MRI thermometry. For example, subject 7 showed a 30% prostate volume reduction from day 0 to day 28 (fig. 3).

Two regions of damage radiated out from the urethra toward the prostate capsule, corresponding to boundaries of thermal necrosis due to ultrasound treatment, with a sharp transition to normal tissue. The first region primarily comprised of fluid filled voids and represented complete thermal cell kill with complete loss of parenchyma and no remaining normal prostate. The second region was interpreted as a narrow transition zone between complete tissue ablation and normal prostatic tissue. It measured a few mm and represented partial thermal cell kill, consisting of fibrosis and some small remnants of normal glandular tissue. In general the urethra was spared from damage within a margin of approximately 1 to 2 mm. These results are in agreement with observations in the literature.¹⁷

Most histology slides showed signs of extensive underlying pathology, such as marked benign glandular hyperplasia and benign complex hyperplasia. This is a normal finding in aging, intact male dogs. In this context normal prostate tissue refers to tissue that was present before study initiation and, thus, not affected by ultrasound treatment.

CE-MRI also confirmed conformal thermal ablation of prostate tissue. Acute CE-MRI (day 0)

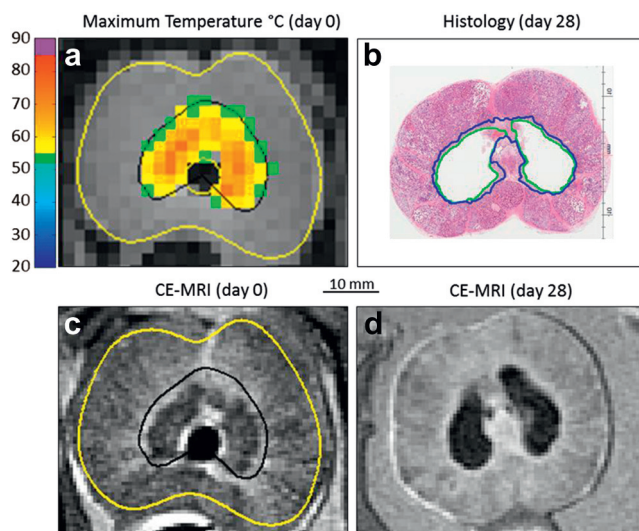


Figure 3. Maximum temperatures produced in prostate (a), thermal cell kill on histology (b), peripheral region of enhancement surrounding NPV on CE-MRI immediately after treatment (c) and NPV on CE-MRI at 28 days (d). At day 0 acute cell kill was confirmed on CE-MRI when peripheral enhanced region surrounding NPV matched 55C maximum temperature isotherm. At 28 days prostate volume was reduced and CE-MRI showed clear NPV matching fluid filled voids on histology. Yellow outline indicates prostate boundary (a and c). Black outline indicates target boundary (a and c). H&E (b).

showed a hypointense NPV surrounded by a peripheral region of hyperintense enhancement, matching the thermal cell kill pattern on MRI thermometry (fig. 3, a and c). This was consistent with previous *in vivo* findings.^{14,15,18} CE-MRI at study completion (day 28) revealed an overall decrease in prostate volume (average 22%, range 11 to 34%) with clear NPV regions at thermal ablation sites. At 28 days no peripheral region of enhancement surrounded the NPV observed on CE-MRI, matching the patterns observed on histology and consistent with a sharp transition to normal tissue (fig. 3, b and d).

Targeting accuracy metrics

Subject No.	Target Accuracy DSC	% Target Accuracy Vol		Target Linear (mm)	
		Over	Under	Accuracy	Precision
1 (multiple technical failures)	0.70	4.2	34.7	-3.1	3.8
2	0.88	0.1	9.1	-1.2	0.8
3	0.86	0.0	9.0	-1.2	0.8
4	0.86	1.5	10.8	-1.2	1.4
5	0.96	0.0	0.2	-0.2	0.5
6	0.89	0.7	9.4	-1.0	1.2
7	0.94	0.0	1.4	-0.5	0.5
8	0.90	1.2	6.3	-0.7	1.0
Av (95% CI)*	0.90 (0.87-0.93)	0.50 (0.0-1.0)	6.6 (3.5-9.7)	-0.9 (-1.2--0.5)	0.9 (0.6-1.2)

* Excluding subject 1.

DISCUSSION

While the canine prostate is the best and most readily available model of the human prostate,²⁵ 2 important limitations impacted this study. The first limitation is that perineal urethrostomy created a large urethral opening just below the anus, which exposed the urethra to fecal contamination. On histology many subjects showed combinations of acute and chronic prostatitis. In the absence of a control group the extent to which fecal contamination contributed to prostatitis independent of treatment could not be elucidated. However, in canines marked prostatitis is a sequela to benign glandular and benign complex hyperplasia. The total extent of inflammation was further confounded by chronic remodeling due to the extensive tissue ablation created by treatment. Additionally, any postoperative bleeding at the perineal urethrostomy wound site resulted in blood contamination of fecal and urine tests.

The second important limitation relates to the physical size of the model. While canine prostate volume (study average 33 cc, range 24 to 44) is comparable to human prostate volume, the overall pelvis is much smaller. In particular the distance between the urethra and the rectum, and between the pelvic bone and the prostate is significantly less. Due to this limitation only subvolume ablation was possible in this long-term chronic safety canine study. Clinically whole gland prostate ablation requires decreasing the margin between the 55C target region and the prostate capsule, which can be done safely due to the accuracy and precision of the treatment. In fact, a prospective, multinational phase I clinical trial is under way to evaluate the safety and feasibility of the TULSA-PRO in patients with localized prostate cancer (ClinicalTrials.gov NCT01686958).²⁶

These results demonstrate the ability to create large conformal volumes of thermal ablation using a single transurethral device with high accuracy and precision in a short time. This is in contrast to other

thermal therapy modalities such as laser, microwave and radio frequency, which have a limited depth of tissue penetration and reduced spatial control of ablation volume. In contrast to transrectal high intensity focused ultrasound, having the transurethral ultrasound heating source in direct contact with the prostate avoids transmitting ultrasound through the rectal wall and allows rapid whole gland prostate ablation. Approximately 30 minutes are required to treat a typical 30 cc prostate. Furthermore, transurethral ultrasound devices are particularly well suited to oncological application because they create large continuous patterns of thermal damage and meet all criteria set out by an international task force on focal treatment of prostate cancer.²⁷ Finally, the nonionizing nature of ultrasound enables repeat treatment, which is desirable in the context of recurrent disease or conservative management of prostate cancer.

CONCLUSIONS

MRI guided transurethral ultrasound therapy is a safe, feasible procedure for accurate and precise conformal prostate ablation. Treatment was well tolerated by all subjects with no clinical adverse events, and normal urinary and bowel function throughout the 28-day followup. Extensive histology confirmed that the ablation region was confined to the prostate and matched MRI thermometry measurements as well as CE-MRI. Using temperature feedback control the intended thermal pattern was generated in vivo with a high level of accuracy and precision on the order of 1 mm. This study meets the objectives set forth to support clinical evaluation of the TULSA-PRO.

ACKNOWLEDGMENTS

Nicole Baker provided quality management. Kee Tang, Matthew Asselin and Michael Wybenga provided technical support.

REFERENCES

1. Ferlay J, Shin HR, Bray F et al: Estimates of worldwide burden of cancer in 2008: GLOBOCAN 2008. *Int J Cancer* 2010; **127**: 2893.
2. Potosky AL, Davis WW, Hoffman RM et al: Five-year outcomes after prostatectomy or radiotherapy for prostate cancer: the prostate cancer outcomes study. *J Natl Cancer Inst* 2004; **96**: 1358.
3. Thompson I, Thrasher JB, Aus G et al: Guideline for the management of clinically localized prostate cancer: 2007 update. *J Urol* 2007; **177**: 2106.
4. Cooperberg MR, Moul JW and Carroll PR: The changing face of prostate cancer. *J Clin Oncol* 2005; **23**: 8146.
5. Neutel CI, Gao RN, Blood PA et al: The changing age distribution of prostate cancer in Canada. *Can J Public Health* 2007; **98**: 60.
6. Chopra R, Colquhoun A, Burtnyk M et al: MR imaging-controlled transurethral ultrasound therapy for conformal treatment of prostate tissue: initial feasibility in humans. *Radiology* 2012; **265**: 303.
7. Diederich CJ and Hynynen K: The development of intracavitary ultrasonic applicators for hyperthermia: a design and experimental study. *Med Phys* 1990; **17**: 626.
8. Lafon C, Koszek L, Chesnais S et al: Feasibility of a transurethral ultrasound applicator for coagulation in prostate. *Ultrasound Med Biol* 2004; **30**: 113.

9. Ross AB, Diederich CJ, Nau WH et al: Highly directional transurethral ultrasound applicators with rotational control for MRI-guided prostatic thermal therapy. *Phys Med Biol* 2004; **49**: 189.
10. Chopra R, Baker N, Choy V et al: MRI-compatible transurethral ultrasound system for the treatment of localized prostate cancer using rotational control. *Med Phys* 2008; **35**: 1346.
11. Burtnyk M, Chopra R and Bronskill MJ: Quantitative analysis of 3-D conformal MRI-guided transurethral ultrasound therapy of the prostate: theoretical simulations. *Int J Hyperthermia* 2009; **25**: 116.
12. Burtnyk M, Chopra R and Bronskill M: Simulation study on the heating of the surrounding anatomy during transurethral ultrasound prostate therapy: a 3D theoretical analysis of patient safety. *Med Phys* 2010; **37**: 2862.
13. Diederich CJ, Stafford RJ, Nau WH et al: Transurethral ultrasound applicators with directional heating patterns for prostate thermal therapy: in vivo evaluation using magnetic resonance thermometry. *Med Phys* 2004; **31**: 405.
14. Chopra R, Tang K, Burtnyk M et al: Analysis of the spatial and temporal accuracy of heating in the prostate gland using transurethral ultrasound therapy and active MR temperature feedback. *Phys Med Biol* 2009; **54**: 2615.
15. Siddiqui K, Chopra R, Vedula S et al: MRI-guided transurethral ultrasound therapy of the prostate gland using real-time thermal mapping: initial studies. *Urology* 2010; **76**: 1506.
16. Partanen A, Yerram NK, Trivedi H et al: Magnetic resonance imaging (MRI)-guided transurethral ultrasound therapy of the prostate: a preclinical study with radiological and pathological correlation using customized MRI-based moulds. *BJU Int* 2013; **112**: 508.
17. Sommer G, Pauly KB, Holbrook A et al: Applicators for magnetic resonance-guided ultrasonic ablation of benign prostatic hyperplasia. *Invest Radiol* 2013; **48**: 387.
18. Boyes A, Tang K, Yaffe M et al: Prostate tissue analysis immediately following magnetic resonance imaging guided transurethral ultrasound thermal therapy. *J Urol* 2007; **178**: 1080.
19. Sapareto S and Dewey W: Thermal dose determination in cancer therapy. *Int J Radiat Oncol Biol Phys* 1984; **10**: 787.
20. Ishihara Y, Calderon A, Watanabe H et al: A precise and fast temperature mapping using water proton chemical shift. *Magn Reson Med* 1995; **34**: 814.
21. Dice L: Measures of the amount of ecologic association between species. *Ecology* 1945; **26**: 297.
22. Yung JP, Shetty A, Elliott A et al: Quantitative comparison of thermal dose models in normal canine brain. *Med Phys* 2010; **37**: 5313.
23. Shattuck DW, Sandor-Leahy SR, Schaper KA et al: Magnetic resonance imaging tissue classification using a partial volume model. *Neuroimage* 2001; **13**: 856.
24. Burtnyk M, N'Djin WA, Kobelevskiy I et al: 3D conformal MRI-controlled transurethral ultrasound prostate therapy: validation of numerical simulations and demonstration in tissue-mimicking gel phantoms. *Phys Med Biol* 2010; **55**: 6817.
25. Roberts WW, Teofilovic D, Jahnke RC et al: Histotripsy of the prostate using a commercial system in a canine model. *J Urol* 2014; **191**: 860.
26. Billia M, Burtnyk M, Kuru T et al: MP62-05 Magnetic resonance imaging (MRI)-guided transurethral ultrasound ablation of prostate cancer: preliminary outcomes of a phase I clinical trial. *J Urol* 2014; **191**: e718.
27. Eggener SE, Scardino PT, Carroll PR et al: Focal therapy for localized prostate cancer: a critical appraisal of rationale and modalities. International Task Force on Prostate Cancer and the Focal Lesion Paradigm. *J Urol* 2007; **178**: 2260.